Elaboration of nanomagnet arrays: organization and magnetic properties of mass-selected FePt nanoparticles deposited on epitaxially grown graphene on Ir(111)

Pierre Capiod, Laurent Bardotti, Alexandre Tamion, Olivier Boisron, Clément Albin, Veronique Dupuis, Gilles Renaud, Philippe Ohresser, Florent Tournus

Elaboration of nanomagnet arrays: organization and magnetic properties of mass-selected FePt nanoparticles deposited on epitaxially grown graphene on Ir(111)

Pierre Capiod,[1] Laurent Bardotti,[1] Alexandre Tamion,[1] Olivier Boisron,[1] Clément Albin,[1] Véronique Dupuis,[1] Gilles Renaud,[2] Philippe Ohresser,[3] and Florent Tournus[1]

[1]*Institut Lumière Matière, UMR5306 Université Lyon 1-CNRS, Université de Lyon, 69622 Villeurbanne cedex, France*

[2]*Univ. Grenoble Alpes, CEA, INAC, MEM, F-38000 Grenoble, France*

[3]*Synchrotron SOLEIL, L'Orme des Merisiers, BP48, Saint-Aubin, 91192 Gif-sur-Yvette, France*

Abstract

The moiré pattern created by the epitaxy of a graphene sheet on an iridium substrate can be used as a template for the growth of 2D atomic or cluster arrays. We observed for the first time a coherent organization of hard magnetic preformed FePt nanoparticles on the 2D lattice of graphene/Ir(111). Nanoparticles of 2 nm diameter have been mass-selected in gas phase and deposited with a low energy on the hexagonal moiré pattern. Their morphology and organization have been investigated using Grazing Incidence Small Angle X-ray Scattering, while their magnetic properties have been studied by X-ray Magnetic Circular Dichroism, both pointing to a FePt cluster/graphene surface specific interaction. The spatial coherence of the nanoparticles is preserved upon annealing up to 700°C where the hard magnetic phase of FePt is obtained.

Nanoparticles are intensively studied for optical[1–4], catalytic[5–7], magnetic[8–12] and storage applications[13–18]. FePt nanoparticles are interesting candidates for ultra-high density storage applications due to their extremely high magnetocrystalline anisotropy when chemically ordered in the $L1_0$ phase[19, 20]. Another requirement for such applications, as well as for fundamental studies, is to organize magnetic nanoparticles in a 2D array. A great effort is devoted to the bottom-up elaboration of periodic patterned arrays of nanoparticles[21–25]. In this domain, the moiré pattern appearing from the epitaxy of graphene (g) on a transition metal has been used successfully to organize by physical vapor deposition (PVD) on g/Ru(0001), g/Cu(111) or g/Ir(111) a wide variety of pure metallic nanoparticles[21, 26–28]. However, organized islands of Fe cannot be grown by PVD on g/Ir(111)[21], so that it is not possible to obtain a superlattice of FePt alloy nanoparticles, even using Pt seeding[26, 29].

The MS-LECBD (Mass-Selected Low Energy Cluster Beam Deposition) technique [30–32] may be used to deposit preformed alloy nanoparticles having a chosen chemical composition. MS-LECBD offers opportunities not accessible by PVD: the cluster size can be controlled and is independent of the surface coverage. Recent studies point out the possibility to organize pure nanoclusters on a graphene moiré using soft-landed clusters of Pt on g/Ir(111) or Pd on g/Ru(0001)[33, 34], where one of the three high-symmetry sites of the surface is more favorable for adsorption. The same approach could enable to order metallic alloys on graphene, and especially hard-magnetic ones ($L1_0$ FePt) with a strong uniaxial magnetization. Such a possibility would rely on a preferential adsorption of deposited particles on specific sites of the moiré superlattice. In order to study the effect of the graphene substrate on FePt particle organization and magnetic properties, we consider here diluted samples, thus avoiding interparticle interactions. In this letter, we report on the low-energy deposition of mass-selected FePt clusters (around 2 nm diameter) on the g/Ir(111) moiré superlattice, and their characterization by GISAXS (Grazing Incidence Small Angle X-ray Scattering) and XMCD (X-ray Magnetic Circular Dichroism). These two complementary experimental techniques allow us to probe respectively the organization and magnetic properties (and hence to detect the chemical ordering phase transition upon annealing) of the FePt nanoparticles. A clear tendency to preferential pining and coherent organization is found, as well as specific properties due to the cluster/surface interaction.

The substrate of graphene on a Ir(111) monocrystal has been prepared using Chemical

Vapor Deposition (CVD) following a procedure well known in the literature[35]. Chemically disordered FePt clusters of 2 nm diameter, synthesized by the MS-LECBD technique, are deposited on the g/Ir(111) surface in a soft-landing regime at various temperatures (see S.M.) with a density of 3×10^4 cluster/µm^2. With this surface coverage and nanoparticle size, a compromise is obtained between a low proportion of multimers[36] and a sufficient signal in X-ray experiments. An amorphous carbon capping layer (a few nanometers thick) is grown after cluster deposition, using carbon wire sublimation under vacuum, to avoid any contamination and sintering.

First, the organization and the nanoparticles morphology have been investigated by GISAXS on the BM32 beamline at ESRF, with an incident X-ray energy of 11 keV and a critical angle of 0.42°. Measurements have been performed on a capped sample, after FePt cluster deposition at 150°C. Once in the beamline UHV chamber, the sample is heated up from room temperature to 700°C.

GISAXS measurements provide information on the lateral correlation, size and shape of the nanoparticles[43–45]. The central intensity reflects the size and shape of the nanoparticles while the correlation peak in the figure 1(a) (highlighted in red) corresponds to the coherent organization of the nanoparticles across the sample. The correlation peak appears only in preferential directions (remarkably in the <100>, <010> and <1-10> directions with the h, k, $l = 0$ surface hexagonal lattice notation), and in the vicinity of $2\theta = 51$ mrad which corresponds to the moiré lattice parameter of 2.53 nm[34, 35, 46]. In other directions (out-of-azimuth), only the central intensity remains. This indicates that, at room temperature, a 2D hexagonal organization of FePt clusters on the moiré lattice, similar to size-selected Pt clusters on g/Ir(111)[34] is obtained, and excludes a simple preferential nearest-neighbor distance. This demonstrates that clusters can diffuse on the surface (since they are initially randomly deposited[47, 48]) before being pinned on specific sites reflecting the moiré periodicity. The cluster/surface interaction is thus favorable for self-organization and may be described as a chemisorption involving π-d hybridization[49] and local re-hybridization from sp^2 carbon to diamond-like sp^3[33]. The sample was then progressively annealed up to 700°C, high enough to promote the FePt $L1_0$ chemical ordering[37, 41]. As seen in figure 1(b), the correlation peak is less intense but a coherent organization still remains. Qualitatively, one can detect moderate changes in the form factor of the particles: the GISAXS signal is more concentrated and intense at low θ angle (near the specular beam).

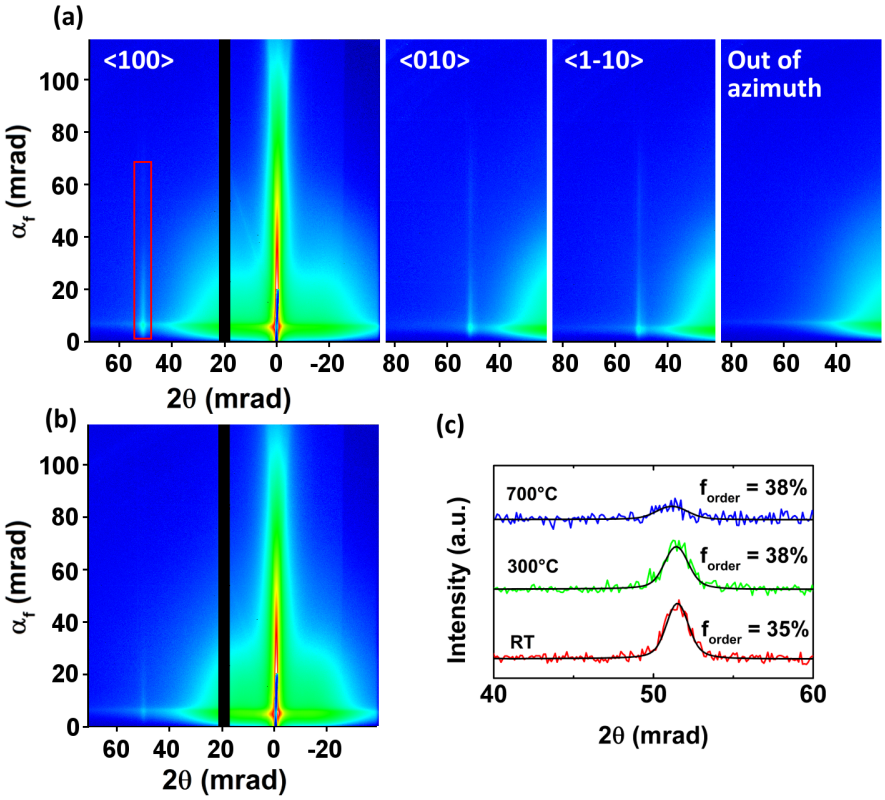

FIG. 1: (a) GISAXS intensities (at room temperature, after deposition at 150°C) along the <100>, <010> and <1-10> directions of the hexagonal moiré lattice. The presence of a correlation peak (highlighted in red) in those directions reflects the hexagonal organization of FePt nanoparticles on the moiré lattice. Out of azimuth, no correlation is visible. (b) GISAXS intensity in the <100> direction at 700°C. (c) GISAXS intensity profile (fixed α_f) of the correlation peak for three different temperatures with their respective fits represented with the black line. The curves have been shifted for clarity. The fraction f_{order} of particles coherently located on the moiré lattice remains constant around 35% ±3%.

A quantitative analysis of the GISAXS patterns (using in-plane and out-of-plane line cuts) gives a precise estimation of the form factor (size and shape) and the lateral correlation of the cluster superlattice. Furthermore, it is possible to link the correlation peak intensity to the proportion f_{order} (supposed to be homogeneous over the entire sample) of nanoparticles coherently pinned on the moiré lattice[34]. The total GISAXS intensity can indeed be separated in two contributions: one coming from particles with random locations[50] on the surface (i.e with no constructive interference and thus no correlation peak) and the other

from organized particles on the moiré lattice.

The incident cluster size deduced from Transmission Electron Microscopy (TEM) observations can be modeled with a gaussian centered on the mean equivalent diameter D_{TEM} = 1.9 nm (see supplementary material). Firstly, we want to determine if the incident particles size is preserved on the surface, since diffusion-coalescence processes could produce larger particles. A first quick analysis of the out-of-azimuth GISAXS cuts, by fitting with a simple gaussian size distribution indicates that the diameter is globally conserved (mean diameter around 1.9 nm), however with a presence of some larger particles (relative dispersion of 50%). In fact, it is not surprising to find a particle size distribution different from the incident monomers because even without diffusion, there is a probability (which depends on the cluster density) that a cluster lands on another one and forms a dimer (or multimers)[53]. If clusters diffuse on the surface, they can form additional multimers. Therefore, we can use a better description to analyze GISAXS measurements using two gaussians: a first one for monomers (main contribution) and a second one corresponding to dimers and multimers. The respective proportion of monomers (X) and dimers (1-X) can be inferred from a best fit, together with the monomers mean size and the dimers relative diameter dispersion[51]. Moreover the particle shape is modeled by truncated spheres with an adjustable H/D ratio, where H is the height and D the in-plane diameter. A value H/D = 0.74, coherent with the wetting parameter found for Pt clusters on g/Ir(111)[34] is obtained. The monomers mean size (spherical equivalent diameter[52]) is found to be D_{eq} = 1.9 nm which is in full agreement with the TEM size histogram while the monomers proportion amounts to 73%. Most of FePt particles on the surface have thus kept their incident size which shows that diffusion, during cluster deposition, is limited but still present. Note that diffusion is indeed required to explain the observed coherent organization and the monomers proportion, slightly lower than expected with a random pinning. Once the size and shape parameters have been determined from the optimal fit of out-of-azimuth GISAXS patterns (see S.M. S3), the proportion f_{order} of particles located on moiré sites is determined from a GISAXS fit along the <100> direction of the moiré lattice. Here the form factors are fixed while the interference function is adjusted (it is directly related to the particle organization i.e. to the moiré crystallographic parameter and the proportion f_{order}[44]).

The intensity of the correlation peak (which depends both on the form factor and on the interference function) and calculated fits are pictured on figure 1(c) for 3 different temper-

atures. At room temperature $f_{\text{order}} = 35\% \pm 3\%$, which is slightly lower but comparable to Pt particles deposited on g/Ir(111) where a value of around 50% is found[34]. This difference is probably due to the larger size of nanoparticles and/or to the alloy nature of FePt clusters. The evolution of the form factor between RT and annealing at 300°C slightly influences the intensity of the correlation peak but f_{order} is in fact almost the same. This is coherent with the fact that at 300°C the temperature is relatively low and does not induce any important changes in the nanoparticles, graphene or amorphous carbon capping layer morphology. Remarkably, at 700°C the organization is preserved and remains visible, with $f_{\text{order}} = 38\% \pm 3\%$. The nanoparticles shape is unchanged, however with a decrease of the monomers proportion down to 65%. At such high temperature, atomic displacements can occur allowing some particles to diffuse over a small distance.

The fact that $f_{\text{order}} < 100\%$ indicates that two types of pinning sites coexist: coherent location(s) within the moiré cell and other positions (incoherent contribution). f_{order} is then linked to the relative density of the different possible pinning sites. However a full description of surface energy potential together with diffusion and coalescence processes is required to infer their density from the f_{order} value, which is out of the scope of this work. Nevertheless, the estimated density of defects in the moiré lattice (moiré domains have sizes in the micrometer range) and/or graphene sheet (wrinkles, step edges...)[35, 54, 55] is too low to account for the proportion of FePt nanoparticles randomly located. This means that clusters landing in some places inside a moiré cell have a non-negligible probability to end up at many various locations (this supposes some kind of rough potential energy landscape, more complex than with only three high-symmetry pining sites), while other landing areas enable the FePt particles to reach specific pinning sites. In order to reach ultra-dense ($>$ 1 Tbit/inch^2) magnetic bit arrays, it is important to understand the pinning mechanisms of preformed clusters as well as the surface energy potential, which governs the diffusion of the nanoparticles on the moiré surface. This may be achieved through theoretical studies or additional experiments (such as STM investigations).

From the GISAXS study, we can tell that the incident particles have been preserved but the surface has a clear influence on their behavior: the random deposition produces, in the end, a partially organized array of particles, even at 700°C. This cluster/surface interaction may as well have an impact on the magnetic properties, which can be investigated by XMCD. Moreover, if chemical ordering has occurred upon annealing, it should be visible through an

evolution of the magnetic properties.

XMCD measurements have been carried out at the DEIMOS beamline at the SOLEIL Synchrotron in Paris-Saclay[40]. By using circularly polarized X-rays, the Fe $L_{2,3}$ edges have been probed using total electron yield (fluorescence mode for the hysteresis loops) for several incidence angles, from normal to the sample (0°) to 60° from normal. Those measurements were investigated from room temperature to low temperature (4 K), before and after annealing of the sample up to 700°C. The sample used for the XMCD characterization, (different from the GISAXS measurements) has been prepared in the same conditions with a higher deposition temperature of 300°C (the organization is identical, see S.M.).

Figure 2(c) shows the hysteresis loops at low temperature (4 K, i. e. in the blocked regime) before (top) and after annealing at 700°C (bottom), for two different X-Ray incidence angles. The hysteresis loops are completely isotropic which shows that there is neither demagnetizing factor effect, nor any preferential orientation of the nanoparticles. Interactions among the 2D layer of nanoparticles (as for a thin magnetic film) or interface anisotropy with the graphene sheet would have introduced an orientation dependence (anisotropy) of the hysteresis loops. Since none has been observed, this is an other evidence that FePt nanoparticles have kept their individuality even after annealing. Note that the magnetic remanence at 4 K is around 50% of the saturation, which is consistent with the model of isolated nanoparticles having a random distribution of their easy axis.

The effect of annealing on the opening of the loops is clear: the coercive field H_C is increasing from 122 mT to 650 mT, reflecting an increase of the magnetic anisotropy constant. From the room temperature magnetization curves (in the superparamagnetic regime, see S.M.), we observe that, as expected, the magnetic size distribution is almost unchanged upon annealing and is in full agreement with the geometrical size distribution deduced from GISAXS. To go further, a theoretical model based on a combined Stoner-Wohlfarth and Néel relaxation description, has been used to fit the hysteresis loops, taking into account the magnetic size distribution[56, 58–61]. A biaxial description has been adopted for the magnetic anisotropy[57], in order to reflect the non ideal morphology of the nanoparticles. Before annealing, the mean anisotropy constant is $K_1 = 300$ kJ/m^3 with a relative dispersion of 40% (we use a gaussian distribution, which reflects the variation of the anisotropy constant among the particles) and a biaxial ratio of $K_2/K_1 = 1.2$.

After annealing, the mean K_1 is 1.4 MJ/m^3 with an increased relative dispersion of 70%

and an unchanged biaxial ratio. This large anisotropy dispersion must be due to a chemical order distribution among the FePt particles, in addition to the existence of a variety of geometries (and possible defects)[37]. The two branches of the hysteresis loop only merge at very high field which implies that some particles in the assembly have an anisotropy field higher than 3 T. We estimate the highest anisotropy constant around 3 MJ/m^3 which is close to the bulk value for $L1_0$ FePt[62, 63]. The value found for the magnetic anisotropy constant is very large for 2 nm FePt nanoparticles, indicating a transition towards the chemically ordered $L1_0$ phase, already observed for particles embedded in a carbon matrix (with possible defects and multiply twinned chemically ordered particles)[37].

Before annealing, the XAS and XMCD measurements depicted on the figure 2(a), show well defined Fe-$L_{2,3}$ absorption edges with no sign of oxidation[64, 65] and a clear magnetic Fe signature. All the spectra have been acquired at the saturation regime, respectively 2 T and 5 T before and after annealing. The maximum intensity of the XMCD spectrum decreases for annealed FePt nanoparticles (figure 2(b)) reflecting a reduced magnetic moment as theoretically expected for $L1_0$ FePt compared to the A1 phase[39, 66].

The Fe magnetic moments (spin and orbital moments, respectively m_S and m_L) have been determined by applying the sum rules[42, 67, 68]. The orbital moment is 0.11 $\pm$0.01 before annealing and decreases to 0.06 $\pm$0.01 after annealing. The spin moment is 3.0 $\pm$0.2 before annealing and 2.5 $\pm$0.2 after annealing. This corresponds to a m_L/m_S ratio of 0.037 $\pm$0.005 before annealing and 0.024 $\pm$0.005 after annealing.

The Fe magnetic moment for the disordered A1 FePt nanoparticles is close to the bulk[69]. Such a high value has never been reported for disordered FePt nanoparticles. Nanoparticles are very sensitive to their environment because of the high surface-to-volume ratio, so that an influence of the graphene on the orbital and spin moments cannot be excluded[70]. After annealing, the spin moment is lower and is similar to the value found in the literature for FePt nanoparticles[38, 66]. However, m_L is surprisingly low compared to previous studies[66, 72], including our results on 3 nm FePt nanoparticles embedded in carbon matrix (0.18 μ_B/at)[38]. m_L is very close to the value of $L1_0$ bulk (0.07 μ_B/at [39, 71]), which is unexpected, since it is usually assumed that the orbital moment in nano-objects is higher than in bulk due to the broken symmetry. Thus it seems that the presence of graphene has a strong effect on Fe orbital moment in the chemically ordered nanoparticles through modification of the electronic structure. The particle flattening and pining, as revealed by GISAXS,

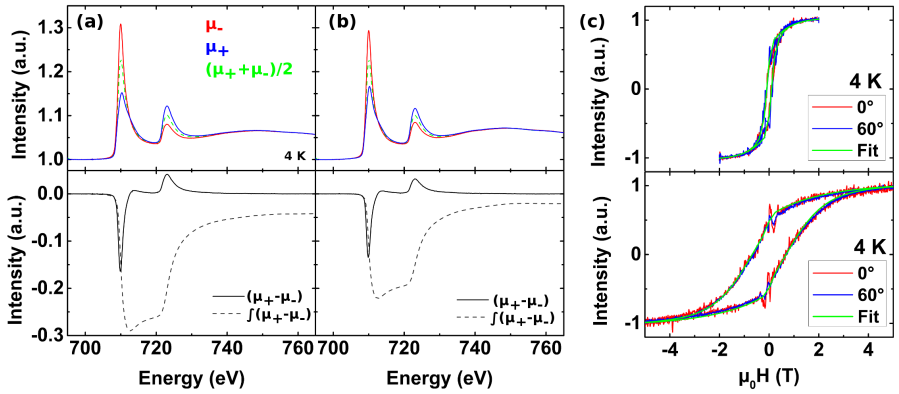

FIG. 2: Top (a) and (b) are respectively before and after annealing XAS spectrum at the Fe $L_{3,2}$ edges taken at 4 K for light circularly polarized left (+) and right (-) with the isotropic XAS signal shown in dotted line. Both averaged XAS signal have been normalized for a direct comparison of the XMCD spectrum. The XMCD spectrum (bottom (a) and (b), respectively before and after annealing) is the difference between the two XAS spectra recorded with opposite orientation of the magnetic field and the x-ray polarization (respectively, blue and red for left and right helicity). The dotted lines are the integral of the XMCD spectrum to highlight the modification of the intensity as well as the evolution of the m_L/m_S ratio. (c) Hysteresis loops taken at 4 K for two incidence angles 0° (normal to the surface, in red) and 60° from the normal (in blue), before annealing (top) and after annealing (bottom). The fits are pictured in green for both phase of the nanoparticles.

imply that a sizeable interaction exist between the FePt clusters and the graphene surface. Charge transfers can occur between the nanoparticles and the graphene and it is very likely to observe a mixing of electronic states as it is observed for clusters and adatoms[73–76]. Magnetic anisotropy energy and orbital moment are closely related: the origin of the MAE comes from the anisotropy of the density of state resulting from the spin-orbit interactions for two distinct directions of the system. The equations derived by Bruno[77], states that for a sizeable contribution to the magnetic anisotropy energy, strong spin-orbit coupling and large orbital moment are needed, which is especially true for the Pt atoms in a FePt alloy. Here, we find that the MAE is not directly proportional to the Fe orbital moment in FePt nanoparticles, in full agreement with theoretical studies[78–81].

In this study, we have reported the organization of size-selected FePt magnetic nanoparticles on a moiré lattice from the epitaxy of graphene on an iridium monocrystal. The

organization has been studied using GISAXS measurements and simulations. We found that after deposition, 38% of the nanoparticles are coherently pinned on the hexagonal moiré lattice. Further theoretical investigation is needed to understand the adsorption energy landscape and the resulting cluster/surface interaction responsible for the organization. A subsequent annealing leads to an impressive increase of the magnetic anisotropy (deduced from XMCD measurements), which can be ascribed to a $L1_0$ chemical ordering transition, while the FePt nanoparticles remain organized on the surface. For the first time, a system made of small FePt nanoparticles, chemically and spatially ordered, has been synthesized and characterized. Moreover we have illustrated that the magnetic anisotropy and the Fe orbital magnetic moment can exhibit a complex relationship and a subtle dependence on interface effects. Future ab-initio calculations may give more insight on the electronic and magnetic interactions between FePt nanoparticles and the g/Ir(111) substrate.

This work is supported by the French state funds Equipex ANR-11-EQPX-0010. The authors acknowledge O. Boisron and C. Albin for their support and assistance at PLYRA. O. Ulrich and F. Choueikani for their help on, respectively, the BM32 beamline at ESRF and the DEIMOS beamline at SOLEIL.

[1] R. Philip, G. R. Kumar, N. Sandhyarani, and T. Pradeep, Phys. Rev. B **62**, 13160 (2000).

[2] R. Jin, Nanoscale **7**, 1549 (2015).

[3] M. Cui, Y. Zhao, and Q. Song, Trends Anal. Chem. **57**, 73 (2014).

[4] J. L. Menendez, B. Bescos, G. Armelles, A. Cebollada, C. Quintana, E. Navarro, R. Serna, J. Gonzalo, C. N. Alfonso, R. Doole, et al., IEEE Trans. Magn. **37**, 1416 (2001).

[5] S. Guo, S. Zhang, L. Wu, and S. Sun, Angew. Chem. **124**, 11940 (2012).

[6] S. Guo and S. Sun, J. Am. Chem. Soc. **134**, 2492 (2012).

[7] L. Xin, F. Yang, S. Rasouli, Y. Qiu, Z.-F. Li, A. Uzunoglu, C.-J. Sun, Y. Liu, P. Ferreira, W. Li, et al., ACS Catal. **6**, 2642 (2016).

[8] S. Sun, S. Anders, T. Thomson, J. E. E. Baglin, M. F. Toney, H. F. Hamann, C. B. Murray, and B. D. Terris, J. Phys. Chem. B **107**, 5419 (2003).

[9] S. Sun, C. B. Murray, D. Weller, L. Folks, and A. Moser, Science **287**, 1989 (2000).

[10] S. M. Binz, M. Hupalo, X. Liu, C. Z. Wang, W.-C. Lu, P. A. Thiel, K. M. Ho, E. H. Conrad,

and M. C. Tringides, Phys. Rev. Lett. **109**, 026103 (2012).

[11] F. Tournus, Phys. Rev. E **84**, 011612 (2011).

[12] T. T. Trung, D. T. Nhung, N. H. Nam, and N. H. Luong, J. Electron. Mater. **45**, 3621 (2016).

[13] C. Chappert, A. Fert, and F. N. Van Dau, Nat. Mater. **6**, 813 (2007).

[14] G. Reiss and A. Hutten, Nat. Mater. **4**, 725 (2005).

[15] J. Hu, J. Chen, and G. Ju, in *Developments in Data Storage* (John Wiley & Sons, Inc., 2011), pp. 223–255.

[16] N. A. Frey, S. Peng, K. Cheng, and S. Sun, Chem. Soc. Rev. **38**, 2532 (2009).

[17] H.-w. Zhang, Y. Liu, and S.-h. Sun, Front. of Phys. in China **5**, 347 (2010).

[18] S. Sun, Adv. Mater. **18**, 393 (2006).

[19] C.-b. Rong, N. Poudyal, G. S. Chaubey, V. Nandwana, R. Skomski, Y. Q. Wu, M. J. Kramer, and J. P. Liu, J. Appl. Phys. **102**, 043913 (2007).

[20] K. Inomata, T. Sawa, and S. Hashimoto, J. Appl. Phys. **64**, 2537 (1988).

[21] A. T. N'Diaye, T. Gerber, C. Busse, J. Mysliveček, J. Coraux, and T. Michely, New J. Phys. **11**, 103045 (2009).

[22] L. Bardotti, F. Tournus, C. Albin, O. Boisron, and V. Dupuis, Phys. Chem. Chem. Phys. **16**, 26653 (2014).

[23] F. Leroy, G. Renaud, A. Létoublon, and R. Lazzari, Phys. Rev. B **77**, 235429 (2008).

[24] F. Leroy, G. Renaud, A. Létoublon, S. Rohart, Y. Girard, V. Repain, S. Rousset, A. Coati, and Y. Garreau, Phys. Rev. B **77**, 045430 (2008).

[25] S. B. Darling, N. A. Yufa, A. L. Cisse, S. D. Bader, and S. J. Sibener, Adv. Mater. **17**, 2446 (2005), ISSN 1521-4095.

[26] J. Coraux, L. Marty, N. Bendiab, and V. Bouchiat, Acc. Chem. Res. **46**, 2193 (2013).

[27] E. Soy, Z. Liang, and M. Trenary, J. Phys. Chem. C **119**, 24796 (2015).

[28] Q. Liao, H. J. Zhang, K. Wu, H. Y. Li, S. N. Bao, and P. He, Nanotech. **22**, 125303 (2011).

[29] C. Vo-Van, S. Schumacher, J. Coraux, V. Sessi, O. Fruchart, N. B. Brookes, P. Ohresser, and T. Michely, Appl. Phys. Lett. **99**, 142504 (2011).

[30] A. Perez, P. Mélinon, V. Dupuis, B. Prével, L. Bardotti, J. Tuaillon-Combes, B. Masenelli, M. Treilleux, M. Pellarin, J. Lermé, et al., Mater. Trans. **42**, 1460 (2001).

[31] A. Perez, V. Dupuis, J. Tuaillon-Combes, L. Bardotti, B. Prevel, E. Bernstein, P. Mélinon, L. Favre, A. Hannour, and M. Jamet, Adv. Eng. Mater. **7**, 475 (2005), ISSN 1527-2648.

[32] A. Perez, P. Melinon, V. Dupuis, L. Bardotti, B. Masenelli, F. Tournus, B. Prevel, J. Tuaillon-Combes, E. Bernstein, A. Tamion, et al., Int. J. Nanotechnol. **7**, 523 (2010).

[33] B. Wang, B. Yoon, M. König, Y. Fukamori, F. Esch, U. Heiz, and U. Landman, Nano Lett. **12**, 5907 (2012).

[34] S. Linas, F. Jean, T. Zhou, C. Albin, G. Renaud, L. Bardotti, and F. Tournus, Sci. Rep. **5**, 13053 (2015).

[35] J. Coraux, A. T. N'Diaye, M. Engler, C. Busse, D. Wall, N. Buckanie, F.-J. M. zu Heringdorf, R. van Gastel, B. Poelsema, and T. Michely, New J. Phys. **11**, 023006 (2009).

[36] With purely random positions, the proportion of monomers (single nanoparticle of the incident size) would be around 80%.

[37] F. Tournus, K. Sato, T. Epicier, T. J. Konno, and V. Dupuis, Phys. Rev. Lett. **110**, 055501 (2013).

[38] V. Dupuis, G. Khadra, S. Linas, A. Hillion, L. Gragnaniello, A. Tamion, J. Tuaillon-Combes, L. Bardotti, F. Tournus, E. Otero, et al., J. Magn. Magn. Mater. **383**, 73 (2015).

[39] P. Andreazza, V. Pierron-Bohnes, F. Tournus, C. Andreazza-Vignolle, and V. Dupuis, Surf. Sci. Rep. **70**, 188 (2015).

[40] P. Ohresser, E. Otero, F. Choueikani, K. Chen, S. Stanescu, F. Deschamps, T. Moreno, F. Polack, B. Lagarde, J.-P. Daguerre, et al., Rev. Sci. Instrum. **85**, 013106 (2014), ISSN 0034-6748.

[41] B. Rellinghaus, S. Stappert, M. Acet, and E. F. Wassermann, J. Magn. Magn. Mater. **266**, 142 (2003).

[42] C. T. Chen, Y. U. Idzerda, H.-J. Lin, N. V. Smith, G. Meigs, E. Chaban, G. H. Ho, E. Pellegrin, and F. Sette, Phys. Rev. Lett. **75**, 152 (1995).

[43] T. H. Metzger, I. Kegel, R. Paniago, A. Lorke, J. Peisl, J. Schulze, I. Eisele, P. Schittenhelm, and G. Abstreiter, Thin Solid Films **336**, 1 (1998).

[44] G. Renaud, R. Lazzari, C. Revenant, A. Barbier, M. Noblet, O. Ulrich, F. Leroy, J. Jupille, Y. Borensztein, C. R. Henry, et al., Science **300**, 1416 (2003).

[45] G. Renaud, R. Lazzari, and F. Leroy, Surf. Sci. Rep. **64**, 255 (2009).

[46] A. T. N'Diaye, S. Bleikamp, P. J. Feibelman, and T. Michely, Phys. Rev. Lett. **97**, 215501 (2006).

[47] F. Tournus, J. Nanopart. Res. **13**, 5211 (2011), ISSN 1572-896X.

[48] F. Tournus, A. Tamion, N. Blanc, A. Hillion, and V. Dupuis, J. Appl. Phys. **109**, 07B502

(2011).

[49] M. Lattelais and M.-L. Bocquet, J. Phys. Chem. C **119**, 9234 (2015).

[50] Truly random positions would produce no correlation peak, but it can also be the case if there are many different sites in the coherently probed zone, which would as well lead to no constructive interference. On the contrary, a statistical occupation of for instance 3 high-symmetry sites would also produce constructive interferences.

[51] The dimers mean diameter is directly related to the one of monomers (by volume conservation) and the relative diameter dispersion of monomers (incident clusters) is fixed to 10%.

[52] The spherical equivalent diameter D_{eq} (sphere of identical volume) of a truncated sphere of parameter H/D is given by $(\frac{D_{eq}}{D})^3 = 3(\frac{H}{D})^2(1-\frac{2}{3}\frac{H}{D})$. In the case of H/D = 0.74, this corresponds to $D_{eq} = 0.94D$.

[53] F. Tournus, N. Blanc, A. Tamion, M. Hillenkamp, and V. Dupuis, J. Magn. Magn. Mater. **323**, 1868 (2011).

[54] N. Blanc, J. Coraux, C. Vo-Van, A. T. N'Diaye, O. Geaymond, and G. Renaud, Phys. Rev. B **86**, 235439 (2012).

[55] J. Coraux, A. T. N'Diaye, C. Busse, and T. Michely, Nano Lett. **8**, 565 (2008).

[56] A. Tamion, E. Bonet, F. Tournus, C. Raufast, A. Hillion, O. Gaier, and V. Dupuis, Phys. Rev. B **85**, 134430 (2012).

[57] A. Thiaville, Phys. Rev. B **61**, 12221 (2000).

[58] M. Jamet, W. Wernsdorfer, C. Thirion, D. Mailly, V. Dupuis, P. Mélinon, and A. Pérez, Phys. Rev. Lett. **86**, 4676 (2001).

[59] M. Jamet, W. Wernsdorfer, C. Thirion, V. Dupuis, P. Mélinon, A. Pérez, and D. Mailly, Phys. Rev. B **69**, 024401 (2004).

[60] A. Tamion, C. Raufast, E. Bonet, V. Dupuis, T. Fournier, T. Crozes, E. Bernstein, and W. Wernsdorfer, J. Magn. Magn. Mater. **322**, 1315 (2010), ISSN 0304-8853.

[61] A. Hillion, A. Tamion, F. Tournus, O. Gaier, E. Bonet, C. Albin, and V. Dupuis, Phys. Rev. B **88**, 094419 (2013).

[62] O. A. Ivanov, L. V. Solina, V. A. Demshina, and L. M. Magat, Phys. Met. Metall. **35**, 81 (1973).

[63] J. M. D. Coey, IEEE Trans. Magn. **47**, 4671 (2011), ISSN 0018-9464.

[64] P. S. Miedema and F. M. F. de Groot, J. Electron Spectrosc. Relat. Phenom. **187**, 32 (2013).

[65] W. Karim, A. Kleibert, U. Hartfelder, A. Balan, J. Gobrecht, J. A. van Bokhoven, and Y. Ekinci, Sci. Rep. **6**, 18818 (2016).

[66] C. Antoniak, J. Lindner, M. Spasova, D. Sudfeld, M. Acet, M. Farle, K. Fauth, U. Wiedwald, H.-G. Boyen, P. Ziemann, et al., Phys. Rev. Lett. **97**, 117201 (2006).

[67] B. T. Thole, P. Carra, F. Sette, and G. van der Laan, Phys. Rev. Lett. **68**, 1943 (1992).

[68] P. Carra, B. T. Thole, M. Altarelli, and X. Wang, Phys. Rev. Lett. **70**, 694 (1993).

[69] C. Antoniak, M. Spasova, A. Trunova, K. Fauth, F. Wilhelm, A. Rogalev, J. Minár, H. Ebert, M. Farle, and H. Wende, J. Phys.: Condens. Matter **21**, 336002 (2009).

[70] W. Q. Liu, W. Y. Wang, J. J. Wang, F. Q. Wang, C. Lu, F. Jin, A. Zhang, Q. M. Zhang, G. van der Laan, Y. B. Xu, et al., Sci. Rep. **5**, 11911 (2015).

[71] I. Galanakis, M. Alouani, and H. Dreyssé, Phys. Rev. B **62**, 6475 (2000), ISSN 0163-1829, 1095-3795.

[72] C. Antoniak, M. Spasova, A. Trunova, K. Fauth, M. Farle, and H. Wende, J. Phys. Conf. Ser. **190**, 012118 (2009).

[73] X. Liu, C.-Z. Wang, H.-Q. Lin, M. Hupalo, P. A. Thiel, K.-M. Ho, and M. C. Tringides, Phys. Rev. B **90**, 155444 (2014).

[74] T. Eelbo, M. Waśniowska, P. Thakur, M. Gyamfi, B. Sachs, T. O. Wehling, S. Forti, U. Starke, C. Tieg, A. I. Lichtenstein, et al., Phys. Rev. Lett. **110**, 136804 (2013).

[75] M. Sargolzaei and F. Gudarzi, J. Appl. Phys. **110**, 064303 (2011).

[76] H. Johll, H. C. Kang, and E. S. Tok, Phys. Rev. B **79**, 245416 (2009).

[77] P. Bruno, Phys. Rev. B **39**, 865 (1989).

[78] I. Galanakis, M. Alouani, and H. Dreyssé, J. Magn. Magn. Mater. **242**, 27 (2002).

[79] I. V. Solovyev, P. H. Dederichs, and I. Mertig, Phys. Rev. B **52**, 13419 (1995).

[80] J. M. MacLaren, R. R. Duplessis, R. A. Stern, and S. Willoughby, IEEE Trans. Magn. **41**, 4374 (2005), ISSN 0018-9464.

[81] Y. Kota and A. Sakuma, J. Phys. Soc. Jpn. **81**, 084705 (2012).